

# Reach Extension of Net-200G/λ IM-DD PAM4 Links to Beyond-100km with Low-complexity Using OE-EQ

Paikun Zhu<sup>1</sup>, Yuki Yoshida<sup>1</sup>, Kouichi Akahane<sup>1</sup>, and Ken-ichi Kitayama<sup>1,2</sup>

1. National Institute of Information and Communications Technology (NICT), Tokyo 184-8795, Japan

2. Hamamatsu Photonics Central Research Laboratory, Shizuoka 434-8601, Japan  
pkzhu3@nict.go.jp

**Abstract:** We report C-band net-202Gb/s/λ IM-DD PAM4 transmission over single-span up-to-100.9km SSMF using only a single-drive intensity modulator, one PD, one ADC, low-complexity DSP and practical FEC, based on a theory-backed optoelectronic equalization (OE-EQ) technique.  
© 2024 The Author(s)

## 1. Introduction

The rapid progression of optical access/edge networks (OAN), mobile X-haul and datacenter interconnects (DCI) [1-3] calls for high-speed and cost-effective optical transmission schemes. While the intensity-modulation direct-detection (IM-DD) scheme still possesses advantages in system simplicity, cost and power consumption for these applications, the data rate should be considerably boosted. For example, considering 6G fronthaul and next-generation OAN, the required rate per wavelength can be 200-Gb/s [1, 2]. Meanwhile, the fiber distance in DCI of major cloud service providers [3] as well as mobile X-haul networks can reach 40km or more. Also, IEEE P802.3dk has started discussion on BiDi optical access of 200-Gb/s over 40km [4]. In these scenarios, a main detrimental issue of high-speed IM-DD transmissions in C-band and even O-band is the power fading induced by fiber chromatic dispersion (CD). To tackle this issue, one way is to switch to coherent technology for signal phase recovery and full CD compensation, including self-coherent or “coherent-lite” techniques [5-9]. Another way is to maintain the phase-recovery-free IM-DD architecture while incorporating anti-fading techniques. For the latter, both optical [10] and electronic [11, 12] techniques have attracted considerable attention. The discussions on digital/electronic approaches were active in recent years due to the increasingly advanced CMOS technology; however, the performance was achieved using relatively complicated digital signal processing (DSP) at the receiver (Rx) and transmitter (Tx).

DD converts the CD channel, a linear all-pass system, to a non-minimum-phase system, resulting in a set of deep notches in the baseband frequency response (BFR), or unstable zeros on the unit circle of the system pole-zero characteristics. This makes the design of a low-complexity inverse system or “equalizer” challenging. We are focusing on a joint opto-electronic equalization (OE-EQ) approach, in which the strategy is to divide the task of anti-fading into 2 parts with simplicity on both sides: a minimal optical circuit removes deep spectral notches in BFR; residual BFR fluctuations are allowed and are compensated by the digital equalizer with greatly-relaxed complexity. A theoretical model of “OE-FFE” (an all-feedforward realization of OE-EQ) was presented [13] with experiments [14].

However, the data rates in previous demonstrations were limited to about 100-Gb/s. It would be important to verify OE-EQ on future-proofing 200G-class IM-DD links and to investigate the required complexity of DSP and the analog hardware. Note that it is much more challenging to tackle 200Gb/s/λ and beyond, since the effect of CD fading scales with the square of the signal bandwidth.

In this work, aided by OE-EQ, we significantly expand the bitrate and distance of C-band IM-DD systems to net-202Gb/s/λ over up-to-100.9km G.652-compliant standard single-mode fiber (SSMF). We demonstrate (1) Tx-side potentially DAC-less operation with a single-drive intensity modulator (IM); (2) Rx includes only a simple and integrable 1-tap optical delay line (ODL) and a single PD; DSP has a relatively low complexity while hard-decision (HD-) FEC [15] or concatenated (C-) FEC [16] can be used.

## 2. Experimental Setup

The experimental setup of OE-EQ-aided net-200G IM-DD transmission is shown in Fig. 1. A 116-GBd electrical

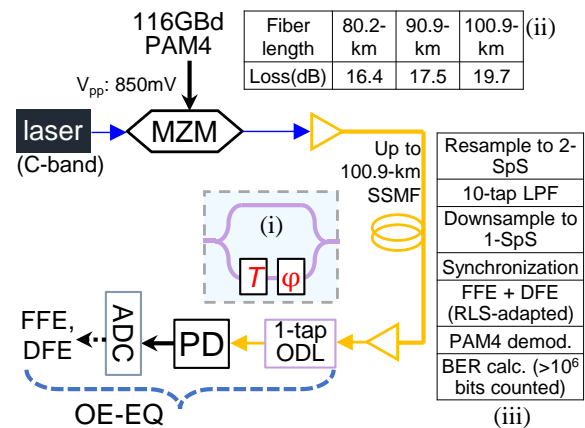


Fig. 1. Experimental setup.  $V_{pp}$ : peak-to-peak voltage. Inset (i): the structure of a 1-tap ODL including two 50:50 couplers, a phase shifter, and a delay component. The optical phase shift  $\phi$  and delay  $T$  are optimizable. The ODL also helped suppress out-of-band ASE. (ii): fiber lengths and corresponding losses. (iii): Rx DSP (from top to bottom). LPF: low-pass filter. RLS: recursive least-square.

PAM4 signal was generated from an arbitrary waveform generator (AWG, Keysight M8199A) outputting 2 samples per symbol (SpS). No Tx DSP was used except a simple pre-distortion of the 4 amplitudes from  $\{-3, -1, 1, 3\}$  to  $\{-3, -0.8, 1.1, 3\}$ . As such, a high-resolution wideband DAC can be omitted in practice. The signal  $V_{pp}$  was 850-mV (i.e., being CMOS-compatible or potentially RF driver-less). The signal was modulated onto an optical carrier ( $\sim 100$ kHz linewidth) at 193.8-THz ( $\sim 1547$ nm) via a single-drive Mach-Zehnder modulator (MZM, 3-dB bandwidth about 30-GHz, half-wave voltage  $V_{\pi,DC}=1.9$ V) biased at the quadrature point. After being amplified to 9-dBm, the optical PAM4 signal was then transmitted over 80.2km, 90.9km or 100.9km SSMF. Fiber lengths were measured by an OTDR. The span losses are listed in the inset (ii). After transmission, an Erbium-doped fiber amplifier (EDFA) compensated for the fiber loss. The PAM4 signal was then processed by a 1-tap ODL (based on free-space optics here but readily implementable on waveguides) with delay ( $T$ ) of 4-ps or free spectral range (FSR) of 250-GHz.  $T$  and  $\varphi$  were optimized guided by the theoretical performance [13];  $T$  is also compatible with standard WDM grid of 50-GHz for future extension to WDM transmission. Subsequently, the signal was power-varied, detected by a 70-GHz PD and captured by a 256GS/s ADC (Keysight oscilloscope). The offline DSP is shown in the inset (iii) of Fig. 1.

### 3. Experimental Results

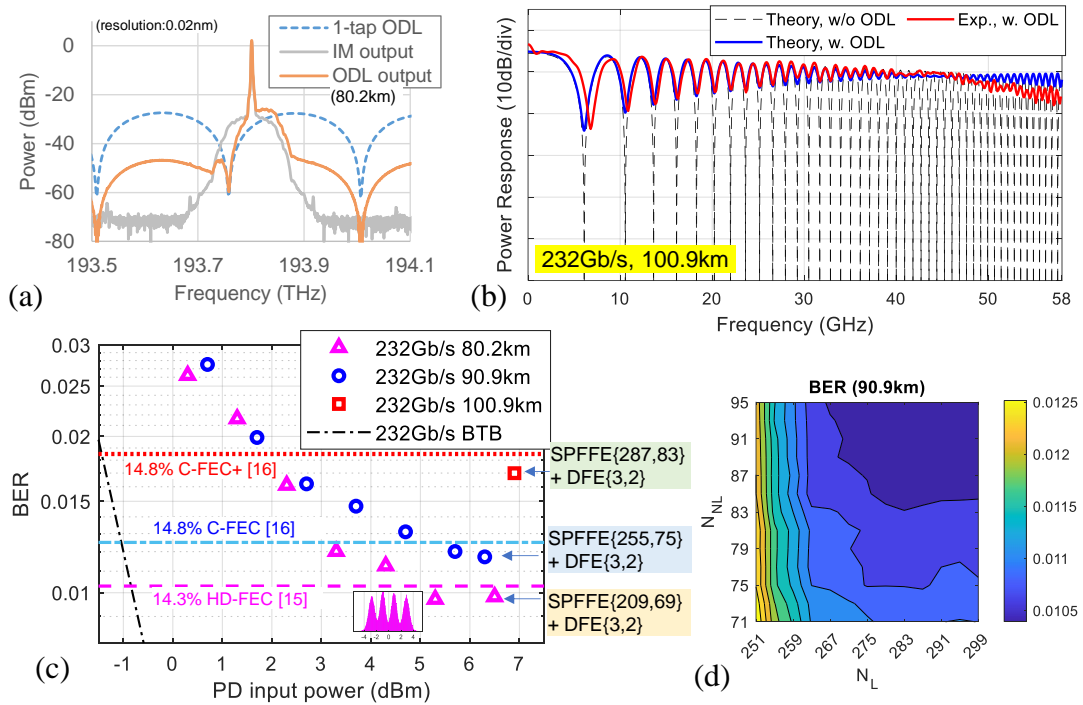


Fig. 2. Experimental results. (a) Optical spectra. (b) Theoretical and experimental (“Exp.”) BFR. (c) BER vs PD input power. The inset shows an amplitude histogram of equalized PAM4 signal (80.2km, +5.3dBm PD input). “SPFFE $\{N_L, N_{NL}\}$ ” means SPFFE with  $N_L$  linear and  $N_{NL}$  nonlinear taps; “DFE $\{N_L, N_{FB}\}$ ” denotes DFE with  $N_L$  feedforward and  $N_{FB}$  feedback taps. (d) Contour plot of BER (90.9km, +6.3dBm PD input) vs.  $N_L$  and  $N_{NL}$  in the SPFFE (cascaded by a fixed DFE $\{3,2\}$ ).

Figure 2(a) shows the optical spectra of the optical PAM4 signal at IM output, at ODL output, and the profile of the 1-tap ODL. Note that the OE-EQ concept is beyond single sideband (SSB) or vestigial sideband (VSB). SSB solves the CD issue by eliminating one sideband, which however requires a complicated Tx. VSB schemes are approximated realizations of SSB, but previously there was no optimization strategy except heuristically approaching the SSB. In contrast, we theoretically reveal that optically removal of critical notches suffices, while a minimal 1-tap ODL suits this task with joint optimization of OE-EQ. Experimentally, we achieve a significant 10-fold bitrate-distance product (BDP) and much lower DSP complexity compared to state-of-the-art net-200G/ $\lambda$  VSB systems [12] (see Fig. 3(a)).

Figure 2(b) shows the BFR (1st Nyquist zone) measured from the received 232Gb/s PAM4 signal after 100.9km transmission. Without the ODL, 45 deep spectral notches caused by CD would occur at frequencies  $f$  satisfying  $\pi\lambda^2 DLf^2/c = (2p-1)\pi/2$  ( $p=1,2,\dots$ ) ( $\lambda$ : wavelength;  $D$ : dispersion coefficient;  $L$ : fiber length;  $c$ : speed of light). Nevertheless, the 1-tap ODL successfully avoided all the deep notches. The residual BFR distortions were handled by the following digital equalizer. Theoretical BFR  $20\log_{10}|H(f)|$  ( $D=16.7$ ps/(nm·km),  $\varphi = -0.65\pi$ ) is also plotted, where

$$H(f) \approx (1 + e^{-j\varphi})(1 + e^{j\varphi} e^{-j2\pi f T})H_{CD}(f) + (1 + e^{j\varphi})(1 + e^{-j\varphi} e^{-j2\pi f T})H_{CD}^*(f) \quad (1)$$

assuming small-signal approximations [17] and ignoring signal-signal beating interference (SSBI);  $H_{CD}(f) = \exp(j\pi\lambda^2 DLf^2/c)$ . (Detailed derivation will be shown on-site due to page limitations.) The experimental BFR

matched well with theoretical prediction. Though the residual notch in BFR could have more than 15dB attenuation, we suggest handling it by cascading a feedforward equalizer (FFE) and a short 2-feedback-tap decision feedback equalizer (DFE), keeping the digital filter ASIC-implementable at 200G throughput [18].

Figure 2(c) depicts the BER versus PD input power with different fiber distances. A 2nd-order simplified polynomial FFE (SPFFE) utilizing absolute operations [13, 19] was applied for a balance between performance and DSP complexity. Notably, complexity of each nonlinear tap in SPFFE is almost the same as that of each linear tap. With cascaded SPFFE [209,69] & DFE [3,2], 14.3% HD-FEC-compliant [15] BER was achieved after 80.2km transmission when the PD input power was 5.3-dBm or higher. For 90.9km and 100.9km reaches, performance met respectively the thresholds of 14.8% C-FEC and C-FEC+ [16] with reasonable power consumption tailored for ZR systems. The net bit rate after removing FEC overheads was 202Gb/s. The penalty in 100.9km case might be reduced by using an EDFA with lower noise for <-10dBm input power, or if a transimpedance amplifier (TIA) were available. The system loss budget is at least 16~19dB if the receiver is defined including the EDFA. If needed, it is also viable to implement SPFFE in the frequency domain [19]. In addition, Fig. 2(d) shows a contour plot of BER versus different number of linear ( $N_L$ ) and nonlinear ( $N_{NL}$ ) taps in SPFFE after 90.9km transmission.  $N_L$  and  $N_{NL}$  can be jointly optimized towards the lowest complexity or the best BER performance.

#### 4. Discussion on the Complexity of DSP and Analog Components

The BDP, estimated DSP complexity and analog component complexity of previous  $\geq$ net-200Gb/s/ $\lambda$  works using IM-DD and self-coherent techniques are shown in Figs. 3(a) and 3(b) respectively. The complexities of DSP modules such as RRC filter, FFE/DFE, Kramers-Kronig (KK) algorithm [22] and CD compensation filter [23] are characterized by the number of (real-valued) multiplications per second (NMPsSec) [24]. The results indicate that the demonstrated OE-EQ-based IM-DD system has a relatively low complexity. Although the required analog device BW were larger than certain prior works, note that ~60GHz-class IM-DD components are generally a baseline to achieve 200G/lane; such components are already in the market and OE-EQ doesn't require more BW than the baseline.

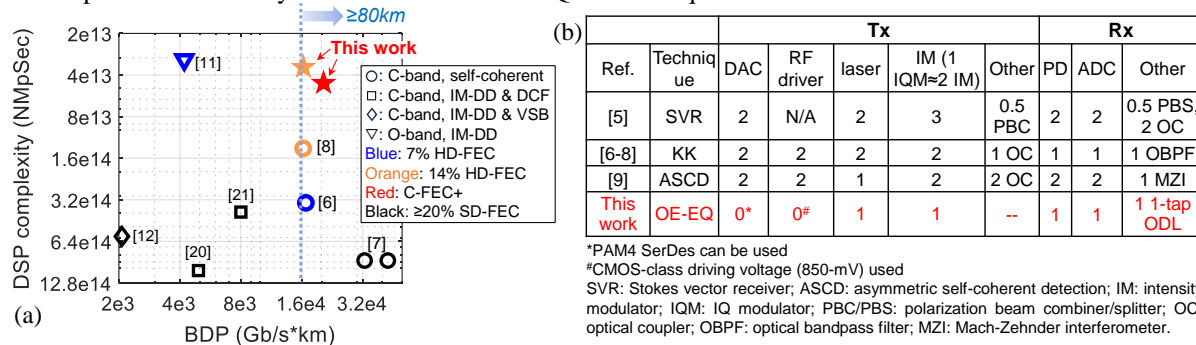


Fig. 3. (a) DSP complexity (in terms of NMPsSec) and bitrate-distance product (BDP) of single-span single-PD  $\geq$ net-200Gb/s/ $\lambda$  demonstrations with disclosed DSP details. DCF: dispersion compensation fiber. (b) Analog complexity of single-span  $\geq$ 80km  $\geq$ net-200Gb/s/ $\lambda$  demonstrations.

#### 5. Conclusion

We have demonstrated C-band DCF-free IM-DD transmission of 232Gb/s (net-202Gb/s/ $\lambda$ ) PAM4 with a significantly extended reach of 80.2km~100.9km SSMF. Aided by the theory-backed OE-EQ, the analog hardware is as simple as one single-drive IM, a 1-tap ODL, a single-ended PD and 1 ADC. DSP with relatively low complexity and practical HD-FEC or C-FEC can still be used. The OE-EQ subsystem is also readily integrable. The demonstrated system can be promising for IM-DD-based future OAN, mobile X-haul and DCI.

#### 6. References

- [1] J. S. Wey et al., J. Opt. Comm. Netw. 15(7), C1-C8 (2023).
- [2] T. Sizer et al., J. Lightwave Technol. 40(2), 346-357 (2022).
- [3] C. Xie and B. Zhang, Proc. IEEE 110(11), 1699-1713 (2022).
- [4] S. Tan and T. Gui, www.ieee802.org/3/dk/public/2308/3dk\_tan\_2308\_2.pdf
- [5] D. Che et al., Proc. OFC 2018, paper Tu2C.7.
- [6] Y. Zhu et al., J. Lightwave Technol., 35(9), 1557-1565 (2017).
- [7] S. T. Le et al., J. Lightwave Technol. 38(2), 538-545 (2020).
- [8] Q. Wu et al., Proc. OFC 2022, paper M2H.6.
- [9] Y. Hu et al., Proc. ECOC 2022, paper Th3B.6.
- [10] C. R. Doerr et al., J. Lightwave Technol. 22(1), 249-256 (2004).
- [11] M. S.-B. Hossain et al., IEEE PTL 33(5), 263-266 (2021).
- [12] C. Wang et al., IEEE PTL 34(18), 941-944 (2022).
- [13] P. Zhu et al., J. Lightwave Technol. 41(2), 477-488 (2023).
- [14] P. Zhu et al., Proc. OFC 2023, paper W4E.3.
- [15] L. M. Zhang and F. Kschischang, J. Lightwave Technol. 32(10), 1999-2002 (2014).
- [16] W. Wang et al., J. Lightwave Technol. 41(3), 926-933 (2023).
- [17] D. J. F. Barros and J. M. Kahn, J. Lightwave Technol. 28(12), 1811-1820 (2010).
- [18] Y. Lu and Y. Zhuang, www.ieee802.org/3/df/public/22\_02/lu\_3df\_01b\_220215.pdf
- [19] Y. Zhou et al., Opt. Express 31(14), 23086-23094 (2023).
- [20] X. Chen et al., Proc. ECOC 2020, paper Th3A-2.
- [21] H. Yamazaki et al., Opt. Express 27(18), 25544-25550 (2019).
- [22] T. Bo and H. Kim, J. Lightwave Technol. 37(2), 461-469 (2019).
- [23] A. Sheikh et al., J. Lightwave Technol. 34(22), 5110-5117 (2016).
- [24] H. Zeng et al., J. Lightwave Technol. 35(6), 1241-1247 (2017).